Available online at www.sciencedirect.com
ScienceDirect
Journal of Sound and Vibration 319 (2009) 1271–1284
JOURNAL OF SOUND AND VIBRATION
www.elsevier.com/locate/jsvi

An enhanced beam model for constrained layer damping and a parameter study of damping contribution ☆

Zhengchao Xie, W. Steve Shepard Jr.*

Department of Mechanical Engineering, The University of Alabama, 290 Hardaway Hall, Box 870276, Tuscaloosa, AL 35487, USA

Received 17 August 2007; received in revised form 23 June 2008; accepted 26 June 2008
Handling Editor: S. Bolton
Available online 23 August 2008

Abstract

An enhanced analytical model is presented based on an extension of previous models for constrained layer damping (CLD) in beam-like structures. Most existing CLD models are based on the assumption that shear deformation in the core layer is the only source of damping in the structure. However, previous research has shown that other types of deformation in the core layer, such as deformations from longitudinal extension and transverse compression, can also be important. In the enhanced analytical model developed here, shear, extension, and compression deformations are all included. This model can be used to predict the natural frequencies and modal loss factors. The numerical study shows that compared to other models, this enhanced model is accurate in predicting the dynamic characteristics. As a result, the model can be accepted as a general computation model. With all three types of damping included and the formulation used here, it is possible to study the impact of the structure's geometry and boundary conditions on the relative contribution of each type of damping. To that end, the relative contributions in the frequency domain for a few sample cases are presented.

1. Introduction

Constrained layer damping (CLD) is an effective passive vibration control approach that is often used on beam-like structures. The deformation of the damping layer (core layer) results from the relative movement of the two face layers, with the result of a damped dynamic response. With a wide range of materials available for use as a core layer, structures with relatively large dynamic loss factors can be designed.

Numerous research has been conducted on CLD in beam structures with the vast majority of that work based on the assumption that there is only shear deformation (pure shear) in the core layer. Ross, Ungar and Kerwin (RKU) used a series of equations to formulate the relationship between the motions of the three layers and the structure loss factor for these sandwich beams [1]. Their work assumed that shear deformation in the core layer and the hysteretic behavior of that material in shear is the main source of damping. An effective

☆ A portion of this work was presented at the Fourth Joint Meeting of the Acoustics Society of America and the Acoustics Society of Japan, Honolulu, HI, December 2007.

*Corresponding author. Tel.: +1 205 348 0048; fax: +1 205 348 6419.
E-mail address: sshepard@coe.eng.ua.edu (W.S. Shepard Jr.).

0022-460X/$ - see front matter © 2008 Elsevier Ltd. All rights reserved.
doi:10.1016/j.jsv.2008.06.041

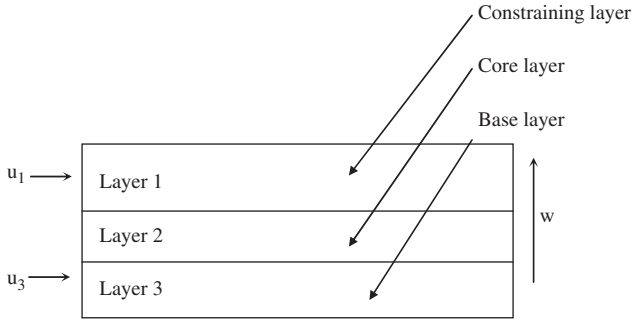

Fig. 1. RKU model displacements for a CLD sandwich beam.

bending stiffness, which is complex due to damping in the core layer, was proposed to be used together with the regular Euler beam model. Later, Mead and Markus [2] proposed a sixth-order differential equation for sandwich beams that can be used for arbitrary boundary conditions. That work was an extension of the RKU model. Both the RKU model and the model developed in Ref. [2] have two common assumptions: (1) the two face layers are treated as Euler beams, and (2) the core layer only experiences shear deformation. The motions associated with these assumptions are illustrated in Fig. 1. For the purposes of this discussion, the two face layers are called the constraining layer and the base layer, while the middle layer is called the core layer. The layers are also denoted by numbers 1, 2 and 3, respectively, throughout this work. The two longitudinal displacements u_1 and u_3 are for the two face layers and w is the transverse displacement, which is the same for all three layers. Shear deformation in the core layer is found from the relative motion between u_1 and u_3. The assumptions described above are widely used.

In some structures, the above assumptions may not always be valid. Rao [3] studied the problem with the same transverse displacement assumption as that in Ref. [1] with the addition that longitudinal displacement varies linearly across the thickness of each layer. Of course, the displacement is continuous across the layer connections. In that work, all three layers are treated as Timoshenko beams instead of the Euler beams used in the RKU model. Rao proposed a system of equations to predict loss factors and natural frequencies of sandwich beams with simply supported boundary conditions. The additional assumptions used in Ref. [3] will be discussed in detail later in this work. The numerical study of Ref. [3] showed that the assumptions in the RKU model that the core layer only experience shear deformation is not accurate in some cases, especially when the core layer is comparatively thick. The analytical models of Refs. [1,3] have one point in common in that all three layers have the same displacement in the transverse direction.

Douglas and Yang [4,5] examined the effect of compressional deformation in the core layer due to the relative transverse displacements of the two face layers. They concluded that damping from the transverse compression deformation of the core layer can be dominant in some cases. Based on this result, Sisemore and Darvennes [6] proposed an eighth-order differential equation in terms of the base layer transverse motion. This equation was developed under the assumption that the two face layers only compress the core layer. No other deformations, such as shear, exist in the core layer. In that work, experimental results were compared with the results from the newly developed equation. It was shown that the model can predict the natural frequencies well. Unfortunately, prediction of the loss factors was not as accurate. This limitation in accuracy is not unexpected since damping from shear deformation, which was completely neglected in that analysis, can often be important. As a result, if only compression deformation is taken into account, loss factors may not be predicted accurately. Sylwan [7] considered the shear and compression damping simultaneously. In that work the core layer was assumed to experience both shear and compressional strain. A set of equations were developed and an iterative scheme used to solve equations to obtain the flexural vibration wavenumbers and loss factors.

When considering the three models that have been mentioned thus far, which hereafter will be referred to as the RKU, RAO, and Sisemore models, respectively, an important question arises: Would the accuracy of loss factor predictions be enhanced if deformations from shear, longitudinal extension, as well as transverse compression were simultaneously included in the model? In the work presented here, an enhanced model is

developed, in which all three of these deformations are taken into account. The advantage of this new formulation is shown by comparing the performance to the Rao model for a range of core layer thickness and stiffness.

One of the unique advantages of this new approach lies in its formulation. Because individual strain energies are used, it becomes possible to track these energies throughout the formulation. As a result, it is now possible to examine the relative contributions of each type of motion to the overall structural damping. A few examples are presented to demonstrate this new capability. With this new tool, designers can now gain more insight into most important design parameters and their impact on vibration reduction performance.

2. Analytical model and application

Prior to introducing the enhanced model, the Rao and Sisemore models need to be reviewed as these models provide a basis for the enhanced model. As noted above, the Rao model [3] was developed under the following assumptions:

(1) The transverse displacements of all three layers are equal.
(2) The longitudinal displacement is linearly distributed across the thickness of each layer.
(3) There is no slip between the layers.

The displacement coordinates for the models based on these assumptions are illustrated in Fig. 2.

Rao used Hamilton's principle to obtain the equations of motion for the sandwich beam. The permitted displacements shown in Fig. 2 were set as generalized coordinates for strain energy and kinetic energy in the beam. All these displacements were treated as harmonic functions that were selected based on the geometric boundary conditions. Substituting these harmonic functions into the equations of motion, the differential equations are converted into algebra equations that are much easier to solve. This same approach will also be used later in this work to obtain an enhanced model.

The assumptions used in the Sisemore model are much different than those used for the Rao model. Sisemore assumed the two face layers are Euler beams and the damping layer is treated as distributed parallel springs, each with complex stiffness, as illustrated in Fig. 3. Due to the different transverse displacements, the two face layers compress or stretch the damped springs, which provide dynamic damping. Although results showed the Sisemore model is poor at predicting loss factors, the effect of compression in the damping layer can still be an important part of the response. On the other hand, the Rao model lacks the effect of transverse

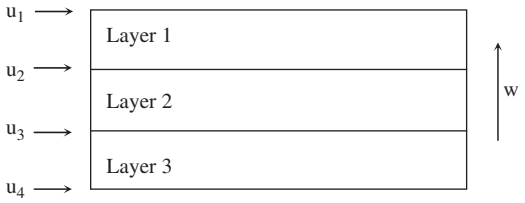

Fig. 2. Rao model displacements for a CLD sandwich beam.

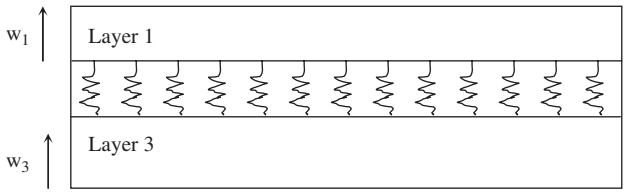

Fig. 3. Sisemore model beam displacements for a CLD sandwich beam.

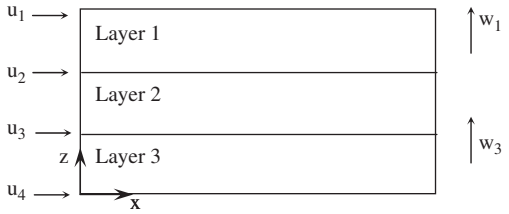

Fig. 4. The enhanced model's beam displacements.

compression on the core layer. Consequently, the following work will combine these effects to obtain an enhanced model.

The enhanced model can be set up with the following assumptions, with the associated coordinates illustrated in Fig. 4:

(1) The transverse displacements of the two face layers are different.
(2) The longitudinal displacement varies linearly across the thickness of each layer.
(3) There is no slip between connected layers.

The first assumption means that the compression deformation of the core layer resulting from relative transverse displacements of the two face layers is included. The second assumption is the same as that of the Rao model in that the effects of both the shear and extension deformations brought by longitudinal displacements of the layers are considered.

With the above assumptions, the strain energy relation can be derived. The kinetic energy can also be obtained in terms of the first-order time derivative of the displacements. As mentioned earlier, the approach in Ref. [3] will be used here, but Lagrange's equation will be used instead of Hamilton's principle.

Based on the assumptions noted above, the displacement vector for the enhanced sandwich beam model is given by

$$\mathbf{u}_{mo} = [\, w_1 \quad w_3 \quad u_1 \quad u_2 \quad u_3 \quad u_4 \,]^{\mathrm{T}}, \tag{1}$$

where w_i is the transverse displacement for the ith layer. As illustrated in Fig. 4, u_1, u_2 and u_3 are the longitudinal displacement for the top surface of layers 1, 2 and 3, respectively, and u_4 is the longitudinal displacement for the bottom surface of the base layer. Because the core layer is compressed by the two outer layers, it follows that

$$w_2 = \frac{w_1 - w_3}{H_2} z + w_3,$$

where H_2 is the thickness of the core layer and z is the coordinate in the transverse direction.

All displacements are treated as harmonic functions, which are selected based on the boundary conditions. The following discussion is for a sandwich beam simply supported at both ends. For other boundary conditions the process is the same and only the basis functions need to be modified. For the simply supported sandwich beam, the transverse and longitudinal displacements will be expressed as follows [3]:

$$w_{im}(x) = \sum_{m=1}^{\infty} W_{im} \sin\left(\frac{m\pi x}{L}\right), \quad i = 1, 3 \tag{2}$$

and

$$u_{jm}(x) = \sum_{m=1}^{\infty} U_{jm} \cos\left(\frac{m\pi x}{L}\right), \quad j = 1, 2, 3, 4, \tag{3}$$

where m is the order of the basis function, W and U are the initially unknown weighting coefficients, x is the location along the beam, and L is the length of the beam.

The kinetic energy for the ith layer is

$$T_i = \frac{1}{2}\int_0^L \rho_i A_i \left(\frac{1}{3}\left(\left(\frac{\partial u_i}{\partial t}\right)^2 + \frac{\partial u_i}{\partial t}\frac{\partial u_{i+1}}{\partial t} + \left(\frac{\partial u_{i+1}}{\partial t}\right)^2 \right) + \left(\frac{\partial w_i}{\partial t}\right)^2 \right) \mathrm{d}x, \tag{4}$$

where t is the time. Note that here and elsewhere the assumed harmonic time dependence is not shown to reduce complexity in the relations. The stain energy for the ith layer is

$$V_i = \frac{1}{6}\int_0^L \left(E_i A_i \left(\left(\frac{\partial u_i}{\partial x}\right)^2 + \frac{\partial u_i}{\partial x}\frac{\partial u_{i+1}}{\partial x} + \left(\frac{\partial u_{i+1}}{\partial x}\right)^2 \right) + 3G_i A_i \left(\frac{\partial w_i}{\partial x} - \frac{u_i - u_{i+1}}{2H_i} \right)^2 + \frac{3E_2 b (w_1 - w_3)^2}{H_2} \right) \mathrm{d}x, \tag{5}$$

where ρ_I, A_i, E_i, G_i and H_i are the ith layer's density, cross-sectional area, Young's modulus, shear modulus, and thickness, respectively. The width of the beam is b.

Substituting the displacement series into Eqs. (4) and (5), Lagrange's equation can then be used to derive the equations of motion. In using this approach, the resulting equations can be found as

$$(\mathbf{K} - \omega^2 \mathbf{M})\mathbf{u}_{mo} = 0, \tag{6}$$

where $\mathbf{M}$ and $\mathbf{K}$ are mass matrix and stiffness matrix, respectively, for the entire structure.

For the simply supported sandwich beam discussed here, the mass matrix is

$$\mathbf{M} = \begin{bmatrix} \rho_1 A_1 + \frac{\rho_2 A_2}{3} & \frac{\rho_2 A_2}{6} & 0 & 0 & 0 & 0 \\ \frac{\rho_2 A_2}{6} & \rho_3 A_3 + \frac{\rho_2 A_2}{3} & 0 & 0 & 0 & 0 \\ 0 & 0 & \rho_1 a_1 & \rho_1 t_1 & 0 & 0 \\ 0 & 0 & \rho_1 t_1 & \rho_1 a_1 + \rho_2 a_2 & \rho_2 t_2 & 0 \\ 0 & 0 & 0 & \rho_2 t_2 & \rho_2 a_2 + \rho_3 a_3 & \rho_3 t_3 \\ 0 & 0 & 0 & 0 & \rho_3 t_3 & \rho_3 a_3 \end{bmatrix} \tag{7}$$

and the stiffness matrix is

$$\mathbf{K} = \begin{bmatrix} \left(\frac{G_2 A_2}{3} + G_3 A_3\right)X^2 + n & \frac{G_2 A_2 X^2}{6} - n & -bG_1 X & \frac{-bG_2}{2}X + bG_1 X & \frac{bG_2 X}{2} & 0 \\ \frac{G_2 A_2 X^2}{6} - n & \left(\frac{G_2 A_2}{3} + G_3 A_3\right)X^2 + n & 0 & \frac{-bG_2 X}{2} & b\left(\frac{G_2}{2} - G_3\right)X & bG_3 X \\ -bG_1 X & 0 & G_1 d_1 + E_1 a_1 X^2 & E_1 t_1 X^2 - G_1 d_1 & 0 & 0 \\ \frac{-bG_2}{2}X + bG_1 X & \frac{-bG_2 X}{2} & E_1 t_1 X^2 - G_1 d_1 & G_1 d_1 + G_2 d_2 + (E_1 a_1 + E_2 a_2)X^2 & E_1 t_1 X^2 - G_1 d_1 - G_2 d_2 & 0 \\ \frac{bG_2 X}{2} & b\left(\frac{G_2}{2} - G_3\right)X & 0 & E_1 t_1 X^2 - G_1 d_1 - G_2 d_2 & G_2 d_2 + G_3 d_3 + (E_2 a_2 + E_3 a_3)X^2 & E_3 t_3 X^2 - G_3 d_3 \\ 0 & bG_3 X & 0 & 0 & E_3 t_3 X^2 - G_3 d_3 & G_3 d_3 + E_3 a_3 X^2 \end{bmatrix} \tag{8}$$

For the geometric variables: $a_i = A_i/3$, $d_i = b/H_i$, $t_i = A_i/6$. Furthermore, $X = \pi m/L$ and $n = E_2 b/H_2$, where L is the length of the beam. Note that for the problems considered here, both the length and width values are the same for all the layers. That is, only full coverage of the damping treatment is considered.

The $\mathbf{K}$ and $\mathbf{M}$ presented above are similar to those given in Ref. [3] with the addition of one degree of freedom, which results from different transverse displacements of the two face layers. $\mathbf{K}$ is complex because the core layer has a complex Young's modulus and shear modulus. The problem can be converted to an eigenvalue problem:

$$\mathbf{K} - \omega^2 \mathbf{M} = 0 \tag{9}$$

The eigenvalues $\omega_i^2 = \omega_i^2(1+\eta_i)$ are complex, where ω_i is the ith natural frequency and η_i is the ith modal loss factor.

Clearly, the difference between the enhanced model and the previous Rao model is that transverse displacements of the face layers can be different in the enhanced model. It is important to understand how this difference affects the accuracy of prediction. It is therefore natural to examine how the thickness and the stiffness of the core layer impact predictions for these two models. In Ref. [3], Rao compared other models with his model and showed better performance with variations in thickness and stiffness of the core layer and the constraining layer. In a similar manner, the following section will discuss the prediction of natural frequencies and loss factors using both the Rao model and the enhanced model for different core layer thickness and stiffness.

3. Numerical cases for analytical models

Before using the enhanced model, this modeling approach should be validated. In results provided by Rikards [8], a 0.27-m-long sandwich beam simply supported on both ends is considered. Five different configurations were studied and further details about each configuration can be found in Ref. [8]. That work showed a good match between the results with Rikards' element and three previous results for beams. Rikards' plate model in that same work was verified with previous experimental results. Consequently, Rikards results can be taken as accurate and used for validating the analytical model in the present work. Table 1 shows a comparison between Rikards's analytical results and the enhanced analytical model used in this work under the same five simply supported configurations. It can be seen that in all cases the new model matches previous results well. Unfortunately, it is not possible to validate the present model with the experimental results provided by Sisemore and Darvennes [6] due to a lack of material properties provided in that work. Furthermore, the boundary conditions considered in that work differ from those considered here. In another work, Xie and Shepard Jr. [9] developed a finite element model that corresponds with the enhanced model developed here. That work provided a comparison of this new finite element model with previous experimental results presented in the work of Leibowitz and Lifshitz [10] for several configurations. For the first mode, the new finite element model differed from the first experimental natural frequency by less than 5% and from the first experimental loss factor by less than 13%, with some cases having errors less than 5%. A comparison

Table 1
Comparison between results of enhanced model and Ref. [8]

Case	Mode	Loss factor			Frequency (rad/s)		
		Rikards analytical results [8]	Current model	% Diff.	Rikards analytical results [8]	Current model	% Diff.
1	1	0.50	0.50	0	878	927	5.6
1	2	0.34	0.34	0	2458	2522	2.6
1	3	0.20	0.20	0	4927	4964	0.8
2	1	0.20	0.19	5.0	1538	1550	0.8
2	2	0.43	0.43	0	4549	4736	4.1
2	3	0.50	0.49	4.0	7929	8354	5.4
3	1	0.11	0.11	0	1643	1645	0.1
3	2	0.31	0.31	0	5456	5568	2.1
3	3	0.45	0.44	2.0	9877	10,300	4.3
4	1	0.32	0.32	0	1106	1132	2.4
4	2	0.20	0.21	5.0	3481	3508	0.8
4	3	0.11	0.11	0	7300	7292	0.1
5	1	0.10	0.10	0	1581	1582	0.1
5	2	0.26	0.26	0	5357	5422	1.2
5	3	0.32	0.32	0	10,187	10,372	1.8

between this new finite element model and the analytical model provided here was then conducted for the present work. The first two natural frequencies for the two modeling approaches differ by at most 0.4%, as shown in Table 2. The first two loss factors differ by at most 0.6%. Because a publication related to Ref. [9] is pending, a detailed validation is not possible until that work becomes available. Based on these comparisons with other approaches, though, it appears that the performance of the current enhanced model is acceptable and can be used in future research.

A comparison between the enhanced model and the Rao model will be made for variations in both the core layer thickness and stiffness for a simply supported beam. For these comparisons, the thickness and stiffness for each of the two face layers will remain constant. In this case, the sandwich beam consists of two aluminum face layers, which are each 0.3 m long, 0.012 m wide and 0.001 m thick. The core layer has the same parameters except for thickness and stiffness, which will be given later. Although the loss factor for viscoelastic materials in general is frequency dependent, it is assumed here to have a constant value of 1 for convenience. Note that this will not be an issue in future use of this method since the emphasis here is to note the difference between the two approaches.

Table 3 shows the comparison for natural frequency and loss factor for the two models with variations of the thickness ratio h, which is defined as the ratio between the core layer thickness and face layers' thickness. In the table, where h varies from 0.05 to 5, the predictions of frequencies and loss factors of the first two modes from the enhanced model and the Rao model are the same.

Table 4 shows the comparison between the two models with variations in the thickness ratio k, which is defined as ratio between Young's modulus for the core layer and Young's modulus of the face layers. As k varies from 10^{-2} to 1, the predictions from two models are still the same.

Table 2
Comparison between the enhanced analytical model and FEA in Ref. [9] for the first two natural frequencies

Thickness (mm)				First mode			Second mode		
Constraining layer	Core layer	Base layer		Enhanced model	FEA [9]	Difference (%)	Enhanced model	FEA [9]	Difference (%)
2	2	2	ω_n	31.8	31.9	0.3	100.5	100.9	0.4
			η	0.380	0.380	0	0.169	0.168	0.6
2	3	2	ω_n	31.5	31.5	0	98.2	98.6	0.4
			η	0.414	0.414	0	0.178	0.177	0.6
2	2	1	ω_n	26.8	26.9	0.4	73.3	73.6	0.4
			η	0.532	0.532	0	0.318	0.316	0.6
2	1	2	ω_n	33.1	33.2	0.3	104.6	105.1	0.5
			η	0.338	0.338	0	0.176	0.175	0.6

Note: 300 mm length with steel face layers.

Table 3
Comparison between the enhanced model and the Rao model with different core layer thicknesses

h		Frequency (rad/s)		Loss factor	
		Rao model	Enhanced model	Rao model	Enhanced model
0.05	Mode 1	327	327	0.003	0.003
0.05	Mode 2	1303	1303	0.011	0.011
0.5	Mode 1	392	392	0.030	0.030
0.5	Mode 2	1496	1496	0.108	0.108
5	Mode 1	752	752	0.263	0.263
5	Mode 2	2127	2127	0.575	0.575

Table 4
Comparison between the enhanced model and the Rao model with different core layer stiffnesses

k		Frequency (rad/s)		Loss factor	
		Rao model	Enhanced model	Rao model	Enhanced model
0.01	Mode 1	469	469	0.007	0.007
0.01	Mode 2	1857	1857	0.026	0.026
0.1	Mode 1	471	471	0.005	0.005
0.1	Mode 2	1883	1883	0.007	0.007
1	Mode 1	479	479	0.037	0.037
1	Mode 2	1918	1918	0.037	0.037

The above discussion illustrates that changing the thickness and stiffness of the core layer will not lead to an apparent difference between the enhanced model and Rao model in the predictions of natural frequencies and loss factors. These identical results can be explained by the fact that shear damping is dominant at the resonant frequencies, and shear damping is included in both models. The importance of the shear damping at these frequencies was also noted in Ref. [6], where it shows that the loss factors calculated from the compression-damping-only model are much smaller than the experimental results. In spite of the dominance of shear damping here, it will be shown below that the compression damping can be dominant in some off-resonant frequency ranges. Regions where this damping cannot be neglected will also be discussed. As mentioned in the previous section of this work, Rao [3] provided some good comparisons between his model and other models. His discussion can be an addition to the comparison in this work to provide a general guidance for the CLD problem.

In the numerical case presented here, it can be seen that compression damping cannot always be neglected. As a result, it is beneficial to investigate the relative contribution of each type of damping. If distributions of each type of damping in a structure are understood, then design engineers can be able to more quickly examine different designs. Because the enhanced analytical model takes all three types of damping into account, it is possible to use the formulation to calculate these relative damping contributions. In the following section the enhanced model is used to calculate the percentages of each type of damping in the total damping.

4. Relative damping contribution formulation

The enhanced model was derived above using the Lagrange equation. In that derivation, the strain energy in all three layers was calculated in Eq. (5). Because the core layer has complex shear and Young's modulus, the strain energy in the core layer is complex and the imaginary component is the energy dissipated by the respective damping. It can be seen that Eq. (5) has three parts including strain energy for extension, shear and compression. All of these are in terms of the six degrees of freedom given in Eq. (1). When the responses of these six degrees of freedom are known, they can be used to calculate the different strain energies in the core layer. In order to calculate the response, Eq. (6) can be changed to

$$(\mathbf{K} - \omega^2\mathbf{M})\mathbf{u}_{mo} = \mathbf{f}. \tag{10}$$

With the displacements in Eqs. (2) and (3), a mode superposition method can be used in Eq. (10) to derive the response at each mode and those summed to obtain the total response. The force used in this study is a unit impulse force applied on the point one-seventh of the length from one end of the beam. Note that in this way the response is in terms of frequency. As a result, the damping distribution will be studied in the frequency domain.

The relative percentage of each type of damping in the total damping is used to illustrate the importance of each damping. The relative percentage of damping can be calculated as

$$P_x = \frac{E_x}{E_c + E_e + E_s} \times 100\% \tag{11}$$

where P_x is the relative percentage, E_e, E_c and E_s are the energy dissipated by extension damping, compression damping and shear damping, respectively. E_x is the energy for the component associated with the percentage of interest. For example, P_s is the percentage of damping associated only with shear.

After the responses are calculated, Eq. (5) is used to calculate the three different components of strain energy. Because the loss factors of shear and Young's modulus are assumed the same and constant, the relative percentages of these three components of strain energy in the total strain energy of the core layer should be the same as the relative percentages of three types of damping in the total damping. The frequency distributions of all three types damping can therefore be found.

5. Relative damping contribution results

If various structure parameters are changed, different distributions of damping may result. Therefore, a parameter study of the relative damping contributions can give some insights regarding the impact of different structural parameters. Because the enhanced model in this work is based on the CLD beam structure, the parameters selected here are beam's length, the core layer thickness, and the two face layers' thicknesses. Note that other parameters, like boundary conditions, could be selected. However, the purpose of this study is only to demonstrate the effectiveness of a new approach. Also the relative damping contribution in other CLD structures such as plates can be studied in the same manner once a suitable analytical plate model which includes all three types of damping is available.

As stated earlier, the beam's length, the core layer thickness and two face layers' thicknesses are selected to study their impact on damping distributions. In the study of each individual parameter the other two parameters are kept constant. All parameters for study of varying beam length, core layer thickness, and the two face layers' thickness are listed in Table 5. The first case is the impact of varying beam length. The beam's length is changed from 200 to 500 mm and other parameters are listed in Table 5. Figs. 5–8 show the impact of different beam lengths on the relative contributions of each type of damping. It can be seen that with longer lengths, shear damping tends to contribute more to the total damping in the low-frequency grange. When frequency is higher than 200 Hz, the compression damping gradually becomes more important and shear damping becomes less important. Note that those frequencies where shear damping reaches a peak are the resonant frequencies of beam's transverse vibration. For extension damping, it can be neglected in most cases for this configuration.

The second case studies the impact of the core layer thickness. The core layer thickness is changed from 2 to 5 mm and other parameters are listed back in Table 5. Figs. 9–12 show the impacts of different core layer thicknesses. It can be seen that damping distributions do not depend much on the core layer thickness. As for the case of the beam length, the compression damping gradually becomes more important and shear damping becomes less important at higher frequency.

Table 5
Parameters used in the three studies on effects of beam length, core layer thickness and two face layers' thicknesses

Parameters	Study	Face layers	Core layer
Thickness (mm)	Beam length	3	3
	Core layer thickness	3	Variable
	Two face layers' thicknesses	Variable	3
Length (mm)	Beam length	Variable	Variable
	Core layer thicknesses	300	300
	Two face layers' thickness	300	300
Width (mm)	All	10	10
Density (kg/m^3)	All	2040	1200
Young's modulus (Pa)	All	45.54E9	0.57E6 $(1+i)$
Shear modulus (Pa)	All	17E9	0.19E6 $(1+i)$

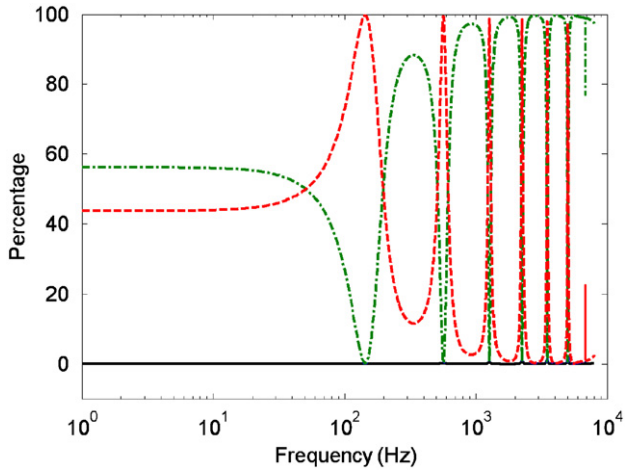

Fig. 5. Damping distribution when beam length is 200 mm (—— extension damping; – · – · compression damping; – – – – shear damping).

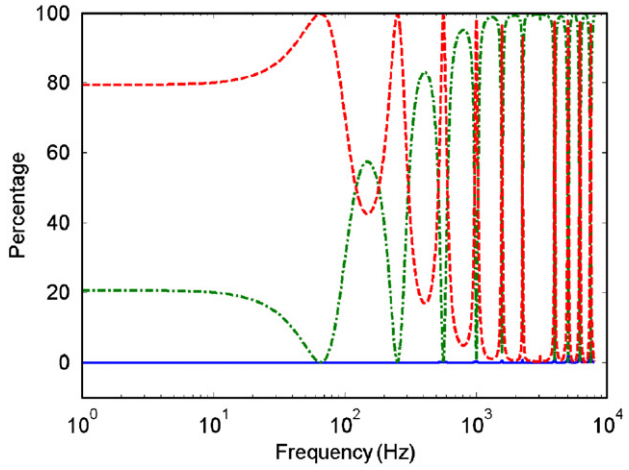

Fig. 6. Damping distribution when beam length is 300 mm (—— extension damping; – · – · compression damping; – – – – shear damping).

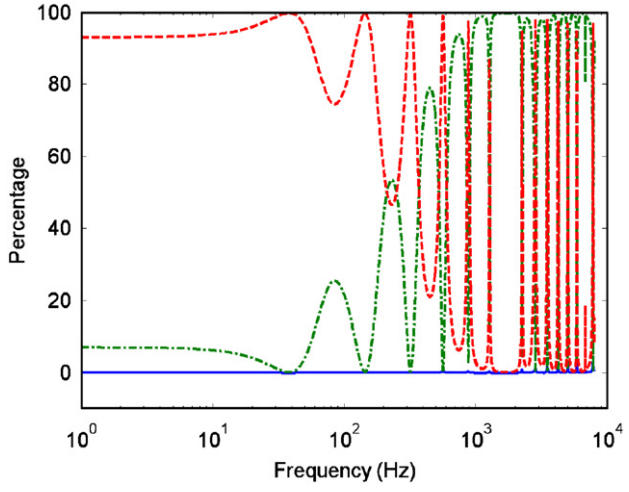

Fig. 7. Damping distribution when beam length is 400 mm (—— extension damping; – · – · compression damping; – – – – shear damping).

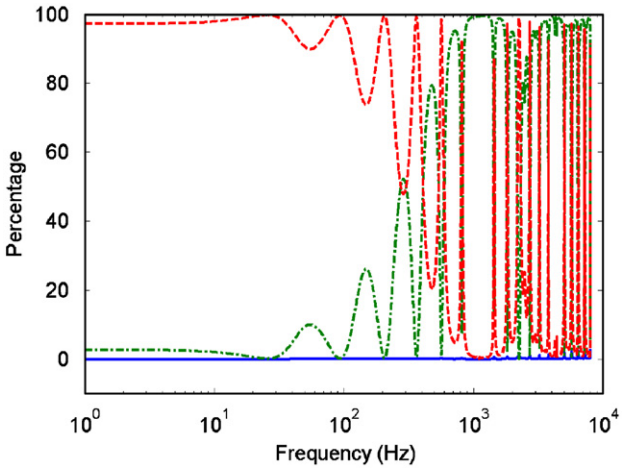

Fig. 8. Damping distribution when beam length is 500 mm (—— extension damping; – · – · compression damping; – – – – shear damping).

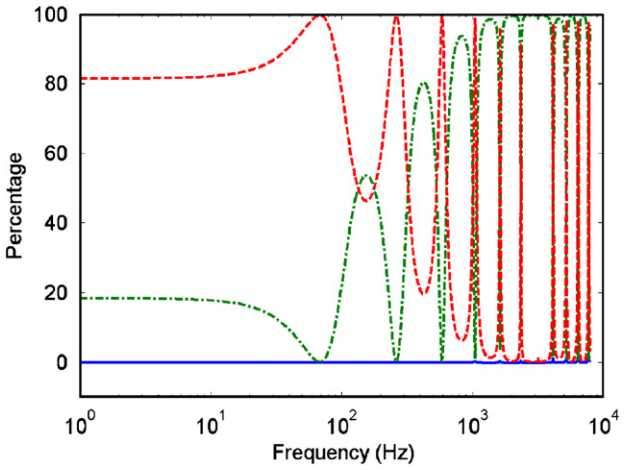

Fig. 9. Damping distribution when the core layer thickness is 2 mm (—— extension damping; – · – · compression damping; – – – – shear damping).

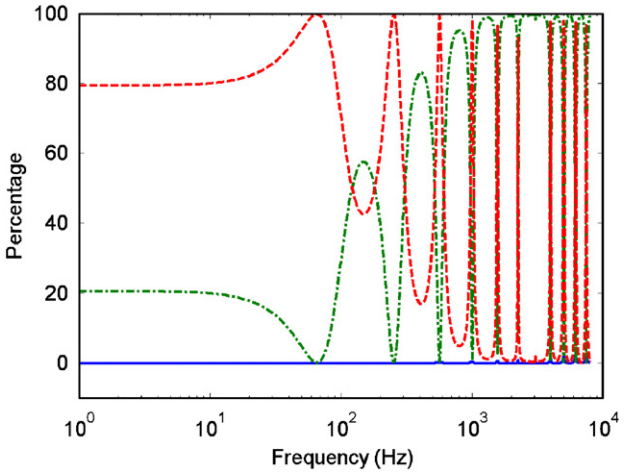

Fig. 10. Damping distribution when the core layer thickness is 3 mm (—— extension damping; – · – · compression damping; – – – – shear damping).

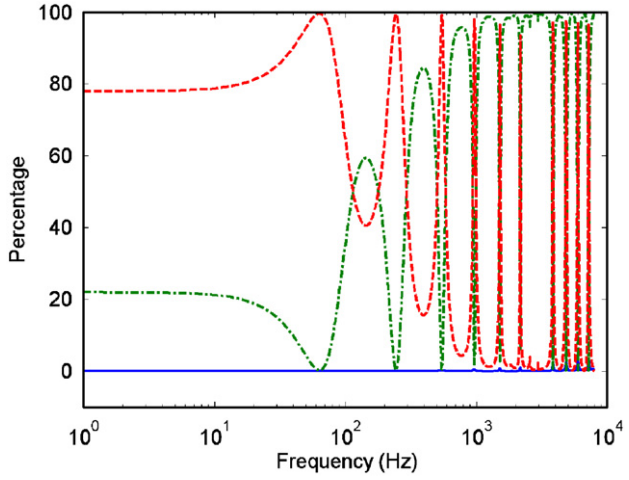

Fig. 11. Damping distribution when the core layer thickness is 4 mm (—— extension damping; – · – · compression damping; – – – – shear damping).

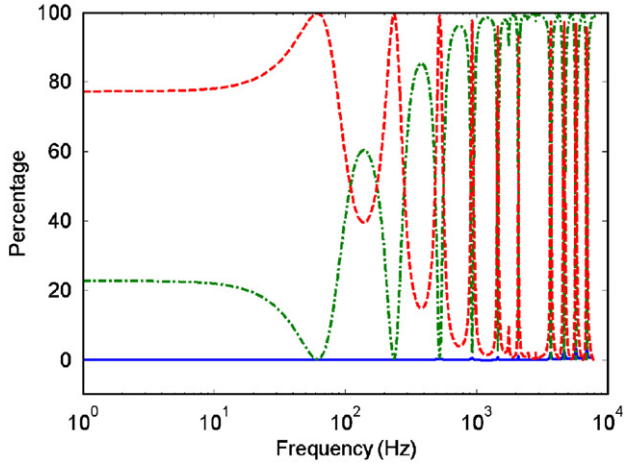

Fig. 12. Damping distribution when the core layer thickness is 5 mm (—— extension damping; – · – · compression damping; – – – – shear damping).

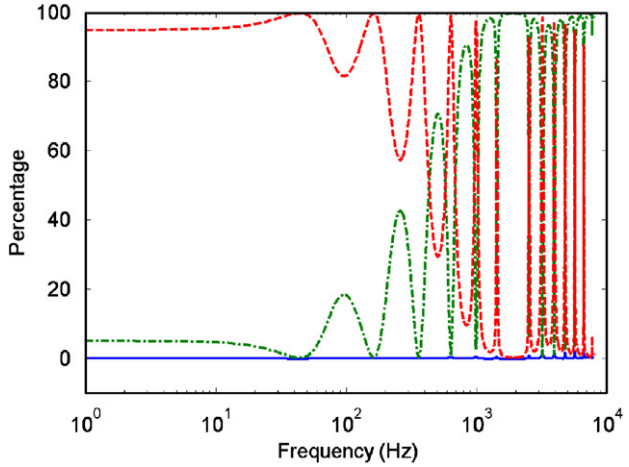

Fig. 13. Damping distribution when two face layers are each 2 mm thick (—— extension damping; – · – · compression damping; – – – – shear damping).

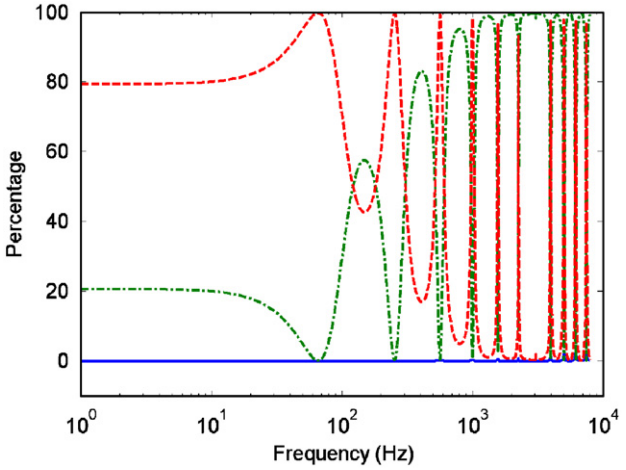

Fig. 14. Damping distribution when two face layers are each 3 mm thick (—— extension damping; – · – · compression damping; – – – – shear damping).

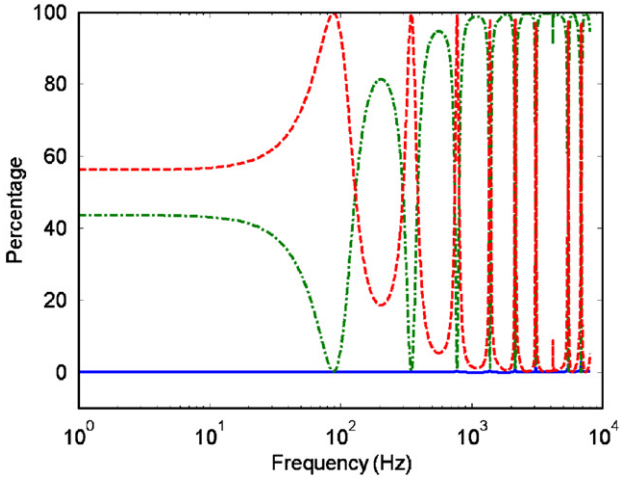

Fig. 15. Damping distribution when two face layers are each 4 mm thick (—— extension damping; – · – · compression damping; – – – – shear damping).

The last case examines the impact of the two face layer thicknesses. Two face layer thicknesses are kept equal and changed from 2 to 5 mm. Other parameters are listed back in Table 5. Figs. 13–16 show the impacts of different face layer thicknesses. It can be seen that the face layers' thicknesses have a great impact on the relative contributions of shear and compression damping, thicker face layers lead to higher contribution of compression damping in the low-frequency range. This is because increases to the face layers' thickness will increase the participation of the compression mode.

6. Conclusion

This work provided the development of an enhanced analytical model for studying structures with CLD. This enhanced model included shear, compression, and extensional damping in the core layer. The numerical examples showed that the enhanced model matches the Rao model when predicting natural frequencies and loss factors. A parameter study on the relative contributions of all three types of damping was conducted using the enhanced model. The parameter study showed that in some cases, particularly at off-resonance conditions,

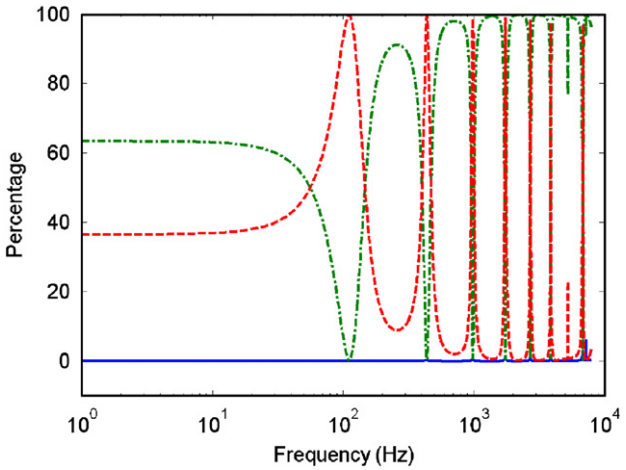

Fig. 16. Damping distribution when two face layers are each 5 mm thick (—— extension damping; – · – · compression damping; – – – – shear damping).

the impact of compression damping can be significant. From the parameter study it was also shown that extension damping usually has little contribution through the whole frequency range and can be neglected in most cases. At the same time longer beam length and lower face layer thicknesses result in a lower relative contribution of compression damping to the total damping, while the core layer thickness has little impact on the damping distributions for the cases studied. These results are not surprising. Based on the study of this work and the work in Ref. [3], a general guidance for the selection of analytical computation models is available for CLD problems.

References

[1] D. Ross, E.E. Ungar, E.M. Kerwin, Damping of plate flexural vibrations by means of viscoelastic laminae, *ASME Annual Meeting on the Structural Damping,* New York, 1959, pp. 49–88.
[2] D.J. Mead, S. Markus, The forced vibration of a three-layer, damped sandwich beam with arbitrary boundary conditions, *Journal of Sound and Vibration* 10 (1969) 163–175.
[3] D.K. Rao, Vibration of short sandwich beams, *Journal of Sound and Vibration* 52 (1977) 253–263.
[4] B.E. Douglas, J.C.S. Yang, Transverse compressional damping in the vibratory response of elastic–viscoelastic–elastic beams, *AIAA Journal* 16 (1978) 925–930.
[5] B.E. Douglas, Compressional damping in three-layer beams incorporating nearly incompressible viscoelastic cores, *Journal of Sound and Vibration* 104 (1986) 343–347.
[6] C.L. Sisemore, C.M. Darvennes, Transverse vibration of elastic–viscoelastic–elastic sandwich beams: compression—experimental and analytical study, *Journal of Sound and Vibration* 252 (2002) 155–167.
[7] O. Sylwan, Shear and compressional damping effects of constrained layer damping, *Journal of Sound and Vibration* 118 (1987) 35–45.
[8] R. Rikards, Finite element analysis of vibration and damping of laminated composites, *Composite Structures* 24 (1993) 193–204.
[9] Z. Xie, W.S. Shepard Jr., A simplified finite-element modeling approach for constrained layer damping, *Journal of the Acoustical Society of America* 122 (2007) 3067.
[10] M.L. Leibowitz, J.M. Lifshitz, Experimental verification of modal parameters for 3-layered sandwich beams, *International Journal of Solids and Structures* 26 (1990) 175–184.